Mem. S.A.It. Vol. 88, 104

Memorie della

Convective overshoot and metal accretion onto white dwarfs

P.-E. Tremblay[1], H.-G. Ludwig[2], B. Freytag[3], D. Koester[4], and G. Fontaine[5]

[1] Department of Physics, University of Warwick, Coventry, CV4 7AL, United Kingdom
e-mail: P-E.Tremblay@warwick.ac.uk
[2] Zentrum für Astronomie der Universität Heidelberg, Landessternwarte, Königstuhl 12, D-69117 Heidelberg, Germany
[3] Department of Physics and Astronomy at Uppsala University, Regementsvägen 1, Box 516, SE-75120 Uppsala, Sweden
[4] Institut für Theoretische Physik und Astrophysik, Universität Kiel, D-24098 Kiel, Germany
[5] Département de Physique, Université de Montréal, C. P. 6128, Succursale Centre-Ville, Montréal, QC, H3C 3J7, Canada

Abstract. A large fraction of white dwarfs host evolved planetary systems and show evidence of accretion from planetary debris. The accretion-diffusion model is the preferred method to understand the metal pollution in these otherwise hydrogen- and helium-rich white dwarf atmospheres. In this scenario, the accreted material first settles on the atmosphere. If the outer stellar layers are unstable to convection, the metals are then rapidly mixed up within the convection zone. In the classical 1D approach, it is generally assumed that the convection zone has a sharp bottom boundary, below which microscopic diffusion is unhampered and slowly removes metals from the visible layers. More realistic 3D radiation-hydrodynamics simulations of white dwarfs with CO5BOLD demonstrate, however, that the bottom of the convection zone does not have a sharp boundary, and that velocities decay exponentially below the unstable convective layers with a velocity scale height of the order of one pressure scale height. This has a potentially dramatic effect on the inferred mass of accreted materiel, hence on the chemical composition and size of planetary debris around white dwarfs.

Key words. convection — stars: interior — white dwarfs

1. Introduction

Post-main-sequence planetary system evolution is now a very active field of research, providing information into their formation, evolution, and fate (Veras 2016). Since the host stars of most known planetary systems will evolve into white dwarfs, it is not surprising that degenerate stars show evidence of evolved planetary systems. A significant number of white dwarfs (>30%) host disrupted minor planets (Farihi et al. 2009; Dufour et al. 2010; Gänsicke et al. 2012; Koester et al. 2014; Vanderburg et al. 2015) and debris disks (~5%). In these systems, the metals detected in spectroscopic analyzes of the otherwise pure-H/He atmospheres provide the bulk composition of disrupted planetesimals, opening a direct window on the properties of rocky exoplanets. Theoretical advances are currently needed to interpret the data, such as the significant differences in time-integrated accretion rates for H- and He-rich atmospheres (Girven et al. 2012).

The majority of white dwarfs polluted by debris have convective atmospheres. The convective turnover timescales are generally very short, hence the metals are fully mixed within the convection zone and slowly diffuse at its base. Most commonly, an approximate approach has been employed with static 1D stellar models coupled with diffusion coefficients and thermal diffusion coefficients (Paquette et al. 1986; Pelletier et al. 1986; Dupuis et al. 1993). It is assumed that the diffusion process takes place in the layers immediately below the base of the 1D convection zone. Recently, there has been numerical and physical improvements to this static method (Fontaine et al. 2015a; Saumon et al. 2015; Paxton et al. 2015). One new approach is to use a time-dependent calculation of the evolution of the abundance profile of an accreting-diffusing element (Fontaine et al. 2015b). This technique has been employed in the evolution code of Brassard & Fontaine (2015), which allows for feedback on the evolving structure from the accreted metals. Additionally, Brassard & Fontaine (2015) were the first to lift the approximation of instantaneous mixing within the convection zone, and instead treat convection as a 1D macroscopic diffusion process. In doing so they have also considered for the first time the effects of non-local convection including overshoot (Freytag et al. 1996) as well as thermohaline mixing (Deal et al. 2013).

So far, all accretion-diffusion studies have employed a version of the empirical 1D mixing-length theory (MLT) of convection (Böhm-Vitense 1958). This is unlikely to change anytime soon as the dynamical time scales for surface convection are orders of magnitude shorter than a typical accretion-diffusion event, suggesting it is currently impossible to simulate both processes simultaneously from the first principles. Nevertheless, our recent 3D radiation-hydrodynamics surface convection simulations of white dwarfs with CO5BOLD (Tremblay et al. 2013) can help in understanding what are the limitations of the 1D MLT model and how the accretion-diffusion model could be improved. In particular, the local 1D MLT approach depicts a simple bottom boundary for a convection zone based on the Schwarzschild stability criterion. In the non-local 3D picture, convective bubbles are still accelerated just before reaching the unstable boundary and the velocities remain significant in overshoot layers located below the classical definition of the convection zone. White dwarf 3D simulations indeed show strong lower overshoot layers (Tremblay et al. 2015).

In this work we attempt to characterize further the impact of non-local convective overshoot on the accretion-diffusion model. In the context of white dwarfs, this effect has so far only been studied in the time-dependent 1D evolution code of Brassard & Fontaine (2015). However, more approximate calculations with static 1D stellar models would also benefit from a parametrization accounting for dynamical convective effects (Koester 2009). We start by reviewing important properties of non-local convection in Section 2 and then concentrate on the effect of convective overshoot at the base of convection zones in Section 3.

2. 3D convection zones

We rely on CO5BOLD 3D simulations that were presented in earlier works (Tremblay et al. 2013, and references therein). The 70 simulations cover the range $6000 \leq T_{\rm eff}$ (K) $\leq 15,000$ and $7 \leq \log g \leq 9$ (see Appendix A of Tremblay et al. 2013). We use a pure-hydrogen equation-of-state and opacity tables that are appropriate for DA white dwarfs (Tremblay et al. 2011). Our simulations cover the full light-emitting layers and are deep enough to include about three pressure scale heights ($H_{\rm P}$) below Rosseland optical depth ($\tau_{\rm R}$) unity. The total size of the convective zone in a DA white dwarf depends on its evolutionary stage. Of particular importance for this work is the regime above 12 000 K at $\log g = 8$, where it is possible to include the full vertical extent of the convectively unstable layers ($\tau_{\rm R} < 1000$) within the 3D simulations. In those cases it is feasible to study directly the properties of the base of the

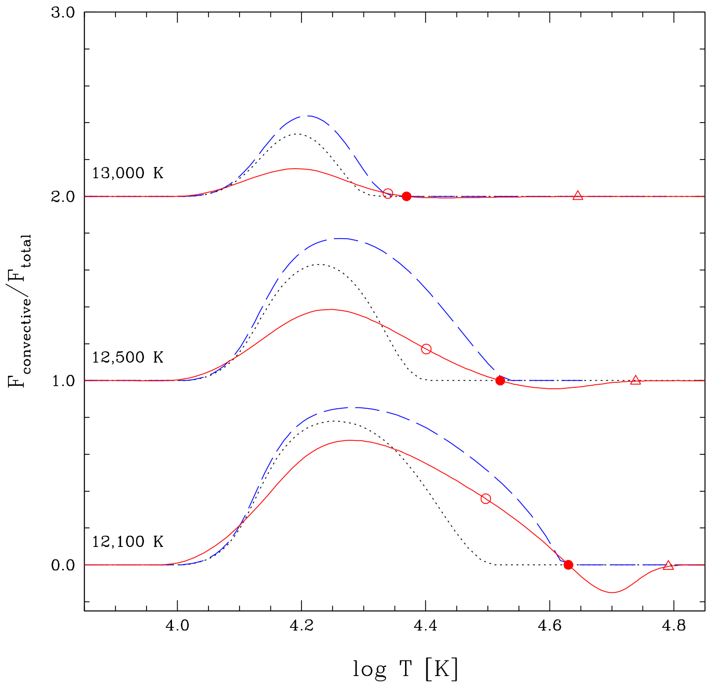

Fig. 1. Ratio of the convective energy flux to total flux as a function of the logarithm of the temperature at $\log g = 8$. The ⟨3D⟩ fluxes are represented by solid red lines and $T_{\rm eff}$ values for the simulations are identified on the panel. The ratio is exact for the 12 100 K model, but the other models are shifted by one for clarity. In order of increasing temperature, we show the position of the stability boundary (open circles), the flux boundary (filled circles), and the $v_{z,\rm rms}$ decay of 1 dex (open triangles) below the value at the flux boundary. We also display 1D model atmospheres matching the stability boundary (black, dotted) and the flux boundary (blue, dashed). Parameters for the stability boundary are ML2/$\alpha_{\rm stab}$ = 0.88, 1.07, and 1.32, for the 12 100, 12 500, and 13 000 K models, respectively. The values are ML2/$\alpha_{\rm flux}$ = 1.00, 1.25, and 1.50 for the flux boundary at the same temperatures.

convection zone. Simulations for cooler DA white dwarfs must instead employ open bottom boundaries and do not include the base of the convection zone. Tremblay et al. (2013) reviewed the predicted spectral properties drawn from these simulations, which mostly depend on the uppermost regions of the convection zone, and the study presented in Tremblay et al. (2015) reported on the overall shape, and in particular the lower part of the convection zone. The latter study is therefore the natural starting point of our present work.

In the following, we rely on mean 3D values, hereafter ⟨3D⟩, for all quantities. ⟨3D⟩ values are the temporal and spatial average of 3D simulations over constant geometrical depth. We use 250 snapshots in the last 25% of a simulation to make the temporal average.

Before comparing 3D simulations and 1D envelopes, it is crucial to define what we refer to as the convection zone. In the local MLT picture, the convective regions are clearly characterized as the layers where the radiative gradient

$$\nabla_{\rm rad} = \left(\frac{\partial \ln T}{\partial \ln P}\right)_{\rm rad} , \tag{1}$$

is larger than the adiabatic gradient

$$\nabla_{\rm ad} = \left(\frac{\partial \ln T}{\partial \ln P}\right)_{\rm ad} , \tag{2}$$

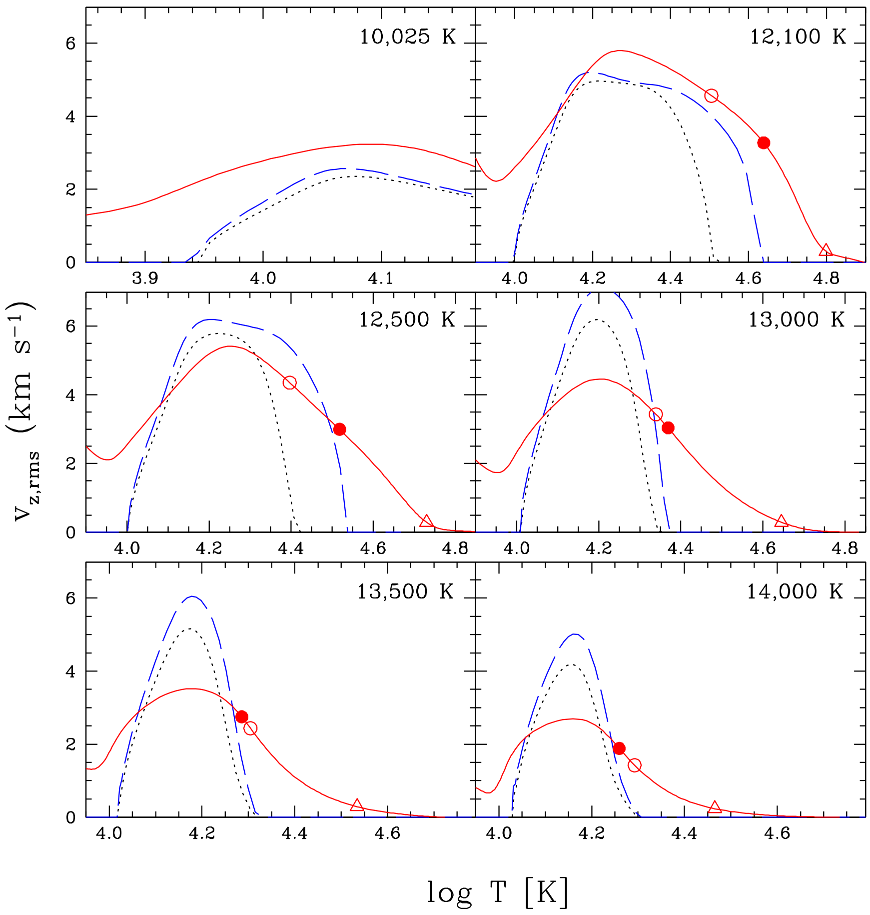

Fig. 2. Vertical RMS velocity as a function of the logarithm of the temperature for 3D simulations at $\log g = 8$ (solid red lines). The $T_{\rm eff}$ values are identified on the top right of the panels. The symbols are the same as in Fig. 1. We also display 1D model atmospheres with the calibration of the MLT parameters for the stability (dotted black) and flux boundaries (dashed blue). For the models warmer than 13 000 K, we rely on an asymptotic parametrization of ML2/$\alpha_{\rm stab}$ = 1.2 and ML2/$\alpha_{\rm flux}$ = 1.4, respectively.

with T the temperature and P the pressure. All other parts of the structure are fully static. This is a rather crude approximation of the dynamical picture of convection, where material flows do not vanish abruptly when the thermal structure becomes stable. In this section, we review the different regions that are found in non-local models of the lower part of convection zones (see also Skaley & Stix 1991; Chan & Gigas 1992; Freytag et al. 1996). Figs. 1 and 2 show the ⟨3D⟩ and 1D convective fluxes and vertical RMS velocity profiles, respectively, for simulations at $\log g = 8$ (Tremblay et al. 2015).

The proper convection zone in 3D (open circles in Figs. 1-2) is defined in the same way as in 1D from the Schwarzschild criterion. Convective flows are largely created, horizontally advected, and merged into narrow downdrafts in the photosphere (Freytag et al. 1996). Large entropy fluctuations are produced by the radiative cooling in these layers, which drives the convective motions. In the following, we define the bottom of this region as the *stability boundary*.

Downdrafts in the immediate vicinity of the lowest unstable layer still have a large momentum. They are also still cooler than the ambient medium. As a consequence, the convective cells are still accelerated in the region just below the unstable layers. The mass conservation guarantees that there is warm material transported upwards, hence there is a positive convective flux is this region. These layers act much like a standard convection zone. We define the bottom of this region as the layer where $F_{\rm conv}/F_{\rm tot} = 0$ and refer to it as the *flux boundary* (filled circles in Figs. 1-2). The typical size of the region between the stability and flux boundaries is a bit less than one pressure scale height, or ~0.3 dex in mass.

At the flux boundary, the momentum of the downdrafts remains significant, hence they penetrate into even deeper layers. This is the beginning of the convective overshoot region. In these layers, convective structures are decelerated since they have a temperature excess and density deficit. As a consequence, they carry a net downwards (negative) convective flux, or in other words, the temperature gradient in these layers is larger than the radiative gradient. However, Fig. 1 demonstrates that this negative overshoot flux is always a small fraction ($\lesssim$ 10%) of the total flux, since the temperature difference between a downdraft and its surroundings is not as large as in the proper convection zone. The overshoot flux decreases approximately in an exponential way with geometrical depth, hence it is not possible to define a strict lower boundary for this region. However, once the convective flux has decreased by one order of magnitude, or to a value of less than 1% of the total flux, the energetic impact becomes very small on the structure.

The negative convective flux and velocities decay in a similar fashion below the flux boundary, with a scale height roughly approximated by $H_{\rm P}$. While the convective flux becomes rapidly energetically negligible, the convective velocities still have mixing capabilities in much deeper layers. This situation is due to the extreme ratio between convective and diffusive time scales. In Figs. 1-2, we identify the position of a 1 dex velocity decay with respect to the velocity at the flux boundary (filled triangles).

Fig. 3 demonstrates that over the three pressure scale heights typically included in our simulations below the flux boundary, the velocity decay is nearly exponential. The velocity scale height is very close to one pressure scale height (dotted black line), although it is actually changing with depth. It is larger than one pressure scale height immediately below the flux boundary, and becomes subsequently smaller.

2.1. Non-local convection in the accretion-diffusion model

Fig. 4 illustrates the different physical processes of interest in terms of their characteristic velocities for a white dwarf envelope at 11 500 K and $\log g$ = 8.0. First of all, we show the 3D convective velocities in solid red (Tremblay et al. 2013), which can be compared to the 1D MLT convective velocities in black (Tremblay et al. 2011). We note that the 3D simulation does not reach the bottom of the convection zone in this case. In comparison, we also show the diffusion velocities for magnesium, calcium, and iron (Koester 2009). It confirms that convective processes are orders of magnitude faster than microscopic diffusion, and that all metals will be completely mixed up within the convection zone.

The 3D simulations only cover the overshoot layers where the velocities decay by about 1-2 orders of magnitude. These layers are well above the deep overshoot regime where microscopic diffusion velocities would be comparable. In other words, if our simulations initially had trace particles within the convection zone, these particles would never reach a sufficient depth below the convection zone for microscopic diffusion to take over. An important word of caution, however, is that overshoot velocities are not the same as diffusion velocities.

The diffusion of particles due to convective overshoot is best studied using tracer particles. Freytag et al. (1996) performed such

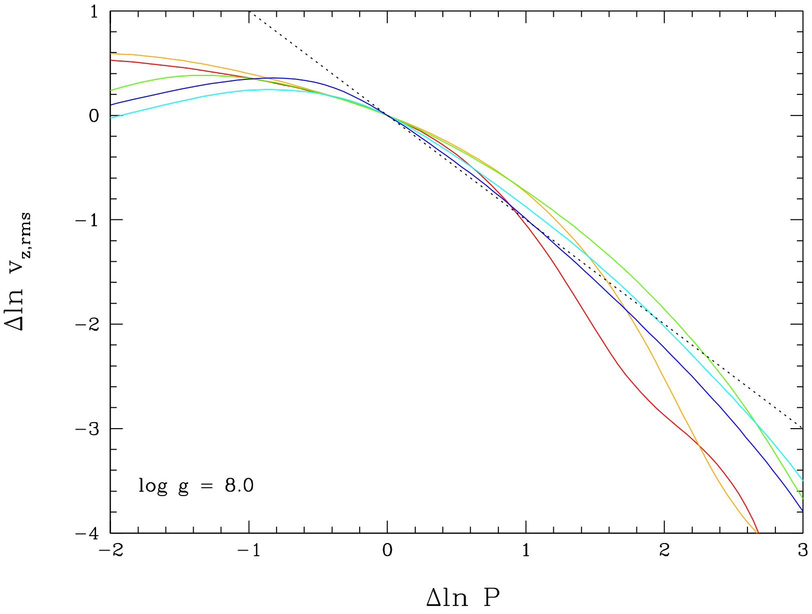

Fig. 3. Vertical RMS velocity decay as a function of pressure (natural logarithm values) for 3D simulations at $\log g = 8$. The reference point is the flux boundary defined as $\Delta \ln v_{z,\mathrm{rms}} = 0$ and $\Delta \ln P = 0$. The simulations are color-coded from 12 100 (red), 12 500 (orange), 13 000 (green), 13 500 (cyan), to 14 000 K (blue). The −1 slope dotted black line represents an exponential velocity decay with a scale height of H_P. The velocity decay at $\Delta \ln P > 2$ could be impacted by the closed bottom boundary condition.

experiments with 2D radiation-hydrodynamics (RHD) simulations of white dwarfs. The results are unlikely to change significantly in 3D, and the 2D approximation allows to reach longer timescales and deeper overshoot layers. Trace particles have no feedback effect on the structure and this represents the case of the accretion of trace amounts of metals in a white dwarf atmosphere. This lack of feedback from the tracers implies that we can not model or verify the efficiency of thermohaline mixing under the presence of an abundance gradient, which may increase the amount of dynamical mixing.

Freytag et al. (1996) found that tracer particles are immediately mixed within the convection zone, but that the RMS vertical spread $\delta z_\mathrm{overshoot}$ in the overshoot layers could be described as

$$\delta z^2_\mathrm{overshoot} = 2D_\mathrm{overshoot}(z)t \;, \tag{3}$$

where $D_\mathrm{overshoot}$ is the macroscopic diffusion coefficient

$$D_\mathrm{overshoot}(z) = v^2_{z,\mathrm{rms}}(z)t_\mathrm{char}(z) \;, \tag{4}$$

with t_char a characteristic timescale. Freytag et al. (1996) demonstrate that the timescale of overshoot is the same as the characteristic convective timescale in the photosphere, since this is where the downdrafts are formed.

In the following we adopt this random walk process characterized by a macroscopic diffusion coefficient to characterize overshoot. This macroscopic diffusion coefficient simply counter-balances the microscopic diffusion coefficient in 1D static envelopes or time-dependent evolutionary calculations. The mixed regions are those where macroscopic diffusion dominates over microscopic diffusion. However, just based on MLT models or even with detailed RHD simulations, $v_{z,\mathrm{rms}}$ is not directly available for the overshoot regions

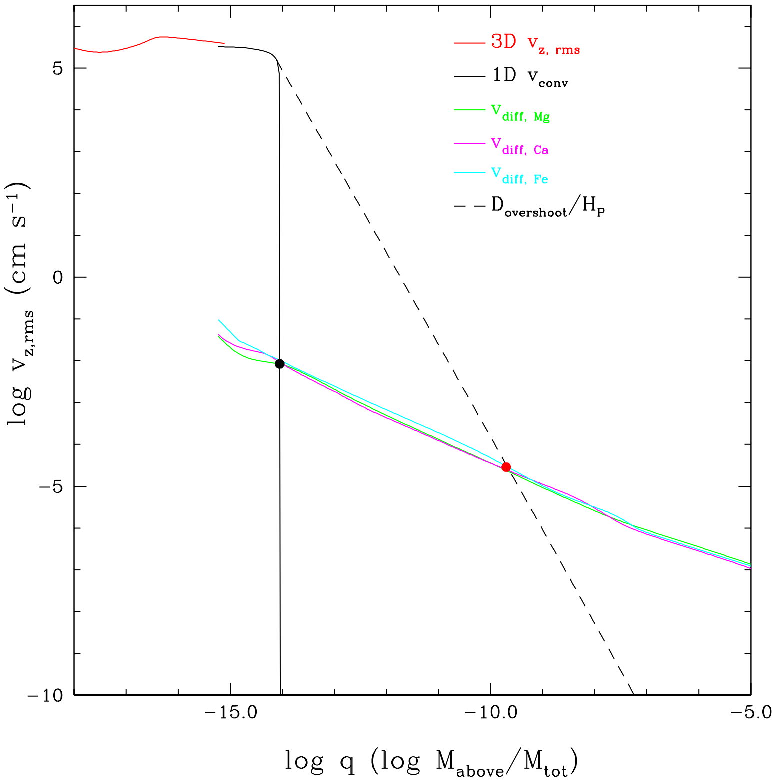

Fig. 4. Characteristic velocities in the envelope of a 11 500 K and $\log g = 8.0$ DA white dwarf as a function of the logarithm of the fractional hydrogen mass. The ⟨3D⟩ vertical RMS velocity (solid red) is compared to the 1D MLT/$\alpha = 0.8$ velocity (solid black). The 3D simulation does not reach the bottom of the convection zone. We also show the microscopic diffusion velocities of Mg, Ca, and Fe in green, magenta, and cyan, respectively. The macroscopic diffusion velocity drawn from Eq. 5 is presented with a dashed line.

of interest, hence the diffusion coefficient is instead estimated from

$$D_{\rm overshoot}(z) = v_{\rm base}^2 t_{\rm char} \exp(2(z - z_{\rm base})/H_{\rm v}) \,, \tag{5}$$

where $v_{\rm base}$ is the velocity at the base of the convection zone and $H_{\rm v}$ the velocity scale height. The results of Fig. 3 suggest that $H_{\rm v} \sim H_{\rm P}$, the latter readily available from 1D envelope calculations. This is admittedly the most uncertain part of our model since it is often required to extrapolate the overshoot velocity decay over many orders of magnitude. We hope that analytical non-local 1D convection models could provide a more physically robust link between the convection zone and deep overshoot layers.

We have transformed the macroscopic diffusion coefficient of Eq. 5 to a velocity using the local pressure scale height as a characteristic dimension as illustrated in Fig. 4 (dashed black line). Once the microscopic diffusion velocities become larger than the macroscopic velocity at the position of the red point, the accreted elements can finally diffuse unhampered towards the interior and leave the extended convection zone. This can be compared to the classical diffusion process that takes place at the position of the black point, just below the classical convection zone. The amount of mass in which the accreted material is mixed is dramatically different between the two scenarios.

The mixed mass increases by up to 3 orders of magnitude when convective overshoot is included.

The results are very similar for the different chemical elements considered in Fig. 4, hence the relative masses of the different accreted elements are not expected to change significantly. We also mention that the parametrization of $v_{\rm base}$ in Eq. 5, whether it is from 1D MLT or 3D models, does not matter much since the extrapolation of the decay of the overshoot velocities assuming $H_{\rm v} \sim H_{\rm P}$ will be the dominant uncertainty to define the region where microscopic diffusion takes place. Our proposed parametrization provides an order of magnitude estimate for applications related to convective mixing in white dwarfs. It is likely to be an upper estimate since for all 3D simulations of Fig. 3, the velocity scale height is slightly smaller than the pressure scale height.

3. Conclusion

We have presented a parametrization of non-local convective effects that can be implemented in the accretion-diffusion model for the accretion of planetary debris onto white dwarfs. The effect of convective overshoot is shown to be important and could increase the inferred mass of accreted debris by 2 to 3 orders of magnitude. For DA white dwarfs, overshoot effects should be included in all cases where there are convective instabilities within the photosphere. For warm temperatures ($14\,000 < T_{\rm eff}$ (K) $< 18\,000$) where the convective flux is negligible, the convective overshoot velocities can still extend to very deep layers and efficiently mix the accreted chemical elements. In the future, we hope to improve our study with a better analytical model of the deep overshoot layers where macroscopic diffusion is very slow and can not be directly simulated from the first principles.

Acknowledgements. This project has received funding from the European Research Council (ERC) under the European Union's Horizon 2020 research and innovation programme (grant agreement No 677706 - WD3D). H.G.L. acknowledges financial support by the Sonderforschungsbereich SFB 881 "The Milky Way System" (subproject A4) of the German Research Foundation (DFG).

References

Chan, K. L., & Gigas, D. 1992, ApJ, 389, L87
Böhm-Vitense, E. 1958, ZAp, 46, 108
Brassard, P., & Fontaine, G. 2015, in 19th European Workshop on White Dwarfs, ed. P. Dufour, P. Bergeron & G. Fontaine (ASP, San Francisco), ASP Conf. Ser., 493 , 121
Deal, M., et al. 2013, A&A, 557, L12
Dufour, P., Kilic, M., Fontaine, G., et al. 2010, ApJ, 719, 803
Dupuis, J., et al. 1993, ApJS, 84, 73
Farihi, J., Jura, M., & Zuckerman, B. 2009, ApJ, 694, 805
Fontaine, G., et al. 2015a, in 19th European Workshop on White Dwarfs, ed. P. Dufour, P. Bergeron & G. Fontaine (ASP, San Francisco), ASP Conf. Ser., 493 , 113
Fontaine, G., et al. 2015b, in 19th European Workshop on White Dwarfs, ed. P. Dufour, P. Bergeron & G. Fontaine (ASP, San Francisco), ASP Conf. Ser., 493 , 117
Freytag, B., Ludwig, H.-G., & Steffen, M. 1996, A&A, 313, 497
Gänsicke, B. T., Koester, D., Farihi, J., et al. 2012, MNRAS, 424, 333
Girven, J., Brinkworth, C. S., Farihi, J., et al. 2012, ApJ, 749, 154
Koester, D. 2009, A&A, 498, 517
Koester, D., Gänsicke, B. T., & Farihi, J. 2014, A&A, 566, A34
Paquette, C., et al. 1986, ApJS, 61, 197
Paxton, B., Marchant, P., Schwab, J., et al. 2015, ApJS, 220, 15
Pelletier, C., et al. 1986, ApJ, 307, 242
Tremblay, P.-E., Bergeron, P., & Gianninas, A. 2011, ApJ, 730, 128
Tremblay, P.-E., Ludwig, H.-G., Steffen, M., & Freytag, B. 2013, A&A, 559, A104
Tremblay, P.-E., Ludwig, H.-G., Freytag, B., et al. 2015, ApJ, 799, 142
Saumon, D., Starrett, C. E., & Daligault, J. 2015, in 19th European Workshop on White Dwarfs, ed. P. Dufour, P. Bergeron & G. Fontaine (ASP, San Francisco), ASP Conf. Ser., 493, 419
Skaley, D., & Stix, M. 1991, A&A, 241, 227
Vanderburg, A., Johnson, J. A., Rappaport, S., et al. 2015, Nature, 526, 546
Veras, D. 2016, Royal Society Open Science, 3, 150571